Hydrogen Bonding of Methanol in Supercritical CO_2 Studied by ^{13}C Nuclear Spin−Lattice Relaxation

Craig M. V. Taylor, Shi Bai, Charles L. Mayne, and David M. Grant*

Department of Chemistry, University of Utah, Salt Lake City, Utah 84112

Received: December 11, 1996; In Final Form: March 26, 1997[⊗]

A sapphire high-pressure NMR cell, capable of independently controlling sample pressure, temperature, and concentration, is used to measure ^{13}C spin−lattice relaxation times for dilute methanol in dense carbon dioxide at pressures from 80 to 220 atm and temperatures from 287 to 334 K. These ranges of temperature and pressure provide relaxation data for methanol in both the liquid and supercritical fluid phases of CO_2. The nuclear Overhauser effect (NOE), used for separating the contributions of the dipolar and spin-rotation mechanisms, has also been measured. Spin-rotation relaxation theory, together with proposed hydrogen-bonding models, is used to interpret the experimental data. The partial molar enthalpy changes for hydrogen bond formation agree well with those reported by Smith et al. using FTIR (*J. Am. Chem. Soc.* **1991**, *113*, 8327−8334) and commonly accepted hydrogen bond energies. A large negative change in the partial molar volume arising from hydrogen bond formation in methanol is observed near the critical temperature of the CO_2−methanol mixture.

Introduction

Supercritical fluid (SCF) CO_2 is limited in its ability to dissolve polar molecules, even at high densities. However, in the supercritical fluid phase, solubility of polar species may be altered significantly and in most cases enhanced by the addition of small amounts of modifier compounds.[1] Methanol is a frequently used modifier because it is highly polar and has a relatively low volatility. The phase behavior of methanol is also relatively simple.[2,3] Solvatochromic studies by Smith et al.[4] suggest that, at high methanol concentrations, the local density of this mixed solvent system in the vicinity of a solute molecule is likely to be higher than that in the bulk solution. A FTIR study also by Smith et al.[5] found significant intermolecular hydrogen bonding between methyl alcohol molecules in several supercritical fluids, including SCF CO_2. The theory that hydrogen-bonded complexes form between molecules for typical alcohols in nonpolar liquid solvents is also well accepted.[6,7] An excellent literature review of hydrogen-bonded complex formation between alcohol molecules has been published by Smith *et al*.[5] Although a variety of structures for hydrogen-bonded complexes have been proposed, it appears that a linear dimer and higher cyclic oligomers are the dominant structures in gas, liquid, and supercritical fluid solvents. It is interesting to note that NMR chemical shift measurements[8] of alcohols in nonpolar solvents, coupled with a chemical−physical model, suggest that the tetrameric complex is dominant even with relatively low concentrations of alcohols.

In studies of solvent clustering in SCF, Pfund[9] and Nishikawa[10] demonstrated that small-angle X-ray scattering is an effective experimental method for direct measurement of solvent aggregations. Recently, laser light scattering techniques have also been used in detecting small size aggregations in polymer solution[11] and organometallic systems.[12] NMR nuclear relaxation measurements have been shown to be an effective experimental method for studying important molecular interactions that influence fluid dynamics.[13] This method has been used to study molecular motions under SCF conditions by Jonas et al.[14,15] and Kobayashi et al.[16−18] for a variety of SCF mixtures. Studies in our laboratory have recently explored SCF structures in CO_2−CH_4 mixtures[19] and local solvent density enhancement in the vicinity of alcohol solute molecules in SCF CO_2.[20]

In this study, the ^{13}C nuclear spin relaxation rates are reported for a CO_2−CH_3OH mixture (0.042 mole fraction methanol) at various temperatures and pressures, encompassing both liquid and supercritical fluid phases. The methanol molecule is approximated as a symmetric top so that the spin-rotation tensor, which unfortunately is not available for ^{13}C nuclei in methanol, may be estimated using the experimental chemical shift tensor data that are available. Interactions between the carbon dioxide electric quadrupole and methanol electric dipole appear to induce increased local density of the CO_2 solvent in the vicinity of solute molecules. A 30% local solvent density enhancement in such a mixture has been reported.[20] In this paper, the hydrogen-bonding interactions between methanol molecules in the methanol−CO_2 system are also examined. It is well-known that NMR chemical shift measurements may be used to investigate hydrogen-bonding interactions of alcohols in solution. Here, a hydrogen-bonding model of spin−lattice relaxation rate is used to interpret the experimental spin−lattice relaxation data. This thermodynamic model characterizes such properties as the partial molar enthalpy and partial molar volume involving hydrogen-bonded cyclic oligomer formation. The effects of pressure and temperature on these thermodynamics properties are discussed.

Experimental Section

A sapphire high-pressure NMR cell, incorporating a movable piston inside the cell body to control the sample pressure, has been described previously.[21] It is used to measure ^{13}C spin−lattice relaxation times along with the associated NOE data. High-purity (99.999%) CO_2 was obtained from Air Products Co. The 99% ^{13}C labeled methanol was obtained from Los Alamos National Laboratory. The methanol sample was microdistilled over a molecular sieve to remove trace amounts of water. The CO_2−methanol mixture was prepared by introducing methanol (30 μL) into the sapphire tube prior to assembly of the cell. The cell was then filled with CO_2 to 60 atm at room temperature. Before the cell was placed into the magnet, it was

[⊗] Abstract published in *Advance ACS Abstracts,* May 15, 1997.

S1089-5647(96)04049-7 CCC: $14.00 © 1997 American Chemical Society

agitated until the methanol was well mixed with the liquid CO_2. A ^{13}C spectrum was obtained with gated proton decoupling to suppress the NOE and comparison with the natural abundance CO_2 resonance indicated that the mole fraction of methanol is 0.042. With an autoshimming program,[22] line widths of 0.5 Hz for CO_2 and methanol in the ^{13}C spectra have been achieved.

A standard inversion recovery pulse sequence[23] ($10T_1-\pi-\tau-\pi/2-$Acq) is used to measure spin−lattice relaxation times. A single-exponential function is found to be adequate to fit the magnetization data as a function of delay time τ to obtain the relaxation time constant, T_1. The reproducibility of ^{13}C T_1 measurements is about 5%. The systematic errors, arising from local heating of the sample during acquisition, were minimized by using gated decoupling instead of continuous broad-band decoupling.

The magnitude of the NOE effect is given by[23]

$$\mathrm{NOE(A\{X\})} = I_A^*/I_A^0 \tag{1}$$

where I_A^* is the integrated intensity of a decoupled spectrum with saturation of the nucleus X and I_A^0 is the equilibrium intensity of A in the coupled spectrum. The maximum possible NOE for $^{13}C\{^1H\}$ is 2.988 when ^{13}C and ^1H relax only by the dipolar mechanism.[23] The NOE effect may be determined as a ratio of spectral intensities with the proton decoupling frequency on resonance and off resonance in the proton spectrum. Since the ^{13}C in CO_2 does not exhibit an NOE, its signal intensity is used as a fiducial reference for the methanol carbon. The relative accuracies of NOE values are estimated to be within ±8%. All nuclear spin−lattice relaxation and NOE measurements were carried out on a Varian VXR 500 NMR spectrometer with a Nalorac 10 mm broad-band probe. The variable temperature control unit in the spectrometer was calibrated with the standard temperature calibration samples of methanol and ethylene glycol. Densities of CO_2−methanol at a given temperature and pressure are calculated using the software SF-Solver for analyzing SCF's.[24]

Theory

A. Nuclear Spin−Lattice Relaxation Rates. The possible relaxation mechanisms for ^{13}C nuclei in methanol under our experimental conditions are the dipole−dipole (DD), spin-rotation (SR), and chemical shielding anisotropy (CSA) interactions. The chemical shielding anisotropy contribution to the relaxation rate may be estimated using the expression[23]

$$\frac{1}{T_{CSA}} = \frac{2}{15}\gamma_c^2 B_0^2 \Delta\sigma^2 \tau_c$$

where γ_C is the magnetogyric ratio for ^{13}C, B_0 is the magnetic field strength, and $\Delta\sigma$ is the shielding anisotropy. B_0 is 11.7 T in our case, and $\Delta\sigma$ is found to be ~70 ppm for methanol.[37,38] The reorientational correlation time τ_C for methanol is usually in the range of picoseconds. Using these data, $1/T_{CSA}$ is estimated to be 0.0004 s^{-1}, which is negligibly small compared with $1/T_{SR}$ and $1/T_{DD}$. Therefore, the overall nuclear spin−lattice relaxation rates for ^{13}C in methanol may be expressed as

$$R_1 = R_{SR} + R_{DD} \tag{2}$$

where R_{DD} and R_{SR} are the relaxation rates from DD and SR contributions, respectively. Since only two major relaxation mechanisms are considered here, the relaxation rates from these contributions can be separated by NOE data using the equation

$$\mathrm{NOE} = 1 + \frac{\gamma_H}{2\gamma_c}\frac{R_{DD}}{R_1} \tag{3}$$

where R_1 is the overall spin relaxation rates measured using the inversion−recovery technique and γ_H and γ_C are the magnetogyric ratios for ^1H and ^{13}C, respectively. Dipolar relaxation in methanol mixtures has been reported;[20] the spin-rotation interaction in this system is discussed herein.

B. Nuclear Spin-Rotation Interactions for Symmetric Top Molecules. An oscillating magnetic field, generated by the motion of a rotating molecule, relaxes the nuclear spins through the spin-rotation interaction. For linear and spherical top molecules, spin-rotation relaxation expressions are relatively simple and may be found in a review article by Jameson.[25] If the methanol molecule is approximated as a symmetrical top molecule with one internal degree of freedom associated with rotation of the methyl about its 3-fold axis, the spin-rotation relaxation rates may be expressed as a summation of contributions from the internal (R_{int}) and overall ($R_{overall}$) relaxation rates.[26]

$$R_{SR} = R_{int} + R_{overall} \tag{4}$$

The overall part of the spin-rotation relaxation rate for symmetrical top molecules has been described by Armstrong and Courtney,[27] and it may be simplified as[28]

$$R_{overall} = (2\tau^2/\alpha)C_{eff}^2\tau \tag{5}$$

where $\alpha = \hbar^2/(2kTI_\perp)$ and $I_\perp$ is the perpendicular component of the moment of inertia. τ_J is the effective spin-rotation correlation time. The effective spin rotation constant, C_{eff}, may be expressed as[27]

$$C_{eff}^2 = k_1 C_a^2 + k_2 C_a C_d + k_3 C_d^2 \tag{6}$$

In eq 6, the structure parameters, k_i, are functions of the moments of inertia. From the IR measurements[29] of the moments of inertia for methanol, k_1, k_2, and k_3 are calculated to be 0.7296, −0.3605, and 0.5905, respectively, using the equations given in ref 27. C_a and C_d are the isotropic and anisotropic components of the spin-rotation tensor as follows:

$$C_a = {}^1/_3(C_{xx} + C_{yy} + C_{zz})$$

$$C_d = {}^1/_2(C_{xx} + C_{yy}) - C_{zz} \tag{7}$$

C_{xx}, C_{yy}, and C_{zz} are the spin-rotation tensor components in the principal axis frame, where zz is defined as parallel to the symmetry axis. The effective correlation time, τ_J, for rotational angular momentum changes is, in general, linearly related to the average time between collisions of solute with solvent molecules at low densities.[30]

For internal rotation of a methyl group, relaxation due to spin rotation is given by[31−33]

$$R_{int} = {}^2/_3 C_\parallel^2 IkT\tau_J \tag{8}$$

Spiess et al.[31] suggest that $C_\parallel$ in methanol is similar to the ^{13}C spin-rotation constant in methane, which is experimentally determined to be 14.26 kHz.[34] I is the moment of inertia for the methyl group about its symmetry axis reported as 5.33×10^{-47} kg m^2.[33] The angular momentum correlation time for internal rotation in methanol is reported to be 2.2×10^{-13} s.[33]

Since the calculation of overall spin-rotation correlation time τ_J involves properties of the solvent, such as density, overall molecular motions are solvent dependent. However, the contributions of the internal rotation of the methyl group to the spin-rotation relaxation rates only depend on temperature (cf. eq 8). Equations 4, 5, and 8, theoretically predict the spin-rotation relaxation rates for ^{13}C methanol in CO_2 if experimental conditions, such as temperature and pressure, are known.

C. Spin-Rotation Interaction Tensor Components. To calculate the overall spin-rotation relaxation rates, the spin-rotation interaction tensor components as used in eq 5 must be known. Unfortunately, the spin-rotation tensor of ^{13}C in methanol has not been determined experimentally. The components of the spin-rotation interaction tensor may be estimated from the methanol chemical shift tensor determined using solid-state NMR. The equation[25,35] relating the chemical shift tensor, $\boldsymbol{\sigma}$, and spin-rotation tensor, **C**, is

$$\sigma_{xx}^{N} = \sigma_{xx}^{d} + \sigma_{xx}^{p}$$

$$\sigma_{xx}^{p} = C_{xx}^{N}\frac{m_p}{2m_e g_N G_{xx}} - \frac{e^2}{2m_e c^2}\sum_{N'}\left[\frac{Z_{N'}(\gamma_{N'}^2 + z_{N'}^2)}{r_{N'}^3}\right] \quad (9)$$

where σ_{xx}^{d} and σ_{xx}^{p} are the diamagnetic and paramagnetic shielding, respectively. The rotational constant in the inertial axis system G_{xx} is experimentally determined.[29] The summation depends on the coordinates of all the other nuclei N′ relative to N, the nucleus of interest, also in the inertial axis system. In eq 9 the center of the nucleus whose shielding and spin-rotation tensor are being considered is taken to be the gauge origin. Solving eq 9 for the spin rotation tensor leads to

$$C_{xx}^{N} = \left\{\sigma_{xx}^{N} - \sigma_{xx}^{d} + \frac{e^2}{2m_e c^2}\sum_{N'}\left[\frac{Z_{N'}(y_{N'}^2 + z_{N'}^2)}{r_{N'}^3}\right]\right\}\frac{2m_e g_N G_{xx}}{m_p} \quad (10)$$

where σ_{xx}^{d} is determined with the Flygare approximation:[36]

$$\sigma_{xx}{}^{d} = \sigma(\text{free atom}) + \frac{e^2}{2m_e c^2}\sum_{N'}\left[\frac{Z_{N'}(y_{N'}^2 + z_{N'}^2)}{r_{N'}^3}\right] + \text{higher order corrections} \quad (11)$$

When the higher order correction terms are neglected, one has

$$C_{xx}^{N} = \frac{2m_e g_N G_{xx}}{m_p}[\sigma_{xx}{}^{N} - \sigma(\text{free atom})] \quad (12)$$

where g_N is 1.4044 and σ(free atom) is 260.74 ppm for carbon nuclei.[35] Three different methods are used to calculate the spin-rotation tensor for the ^{13}C nucleus in methanol. They are (1) solid-state experimental chemical shift data substituted into eq 12, (2) chemical shielding from GIAO methods substituted into eq 12, and (3) solid-state experimental data and σ_{xx}^{d} from the CHF option of RPAC8.5 substituted into eq 10. The results, shown in Table 1, generally agree well with one another. The results of method 2 are entirely ab initio calculations. Method 1 involves the approximation of neglecting higher order correction terms. Method 3 mixes experimental and ab initio calculations and operationally includes the higher order corrections indicated in eq 11. The results (4.99, 4.51, 14.23 kHz) of method 3 are used in this paper because this set of data is closer to that obtained in method 2. It is necessary to note that the spin-rotation tensor components calculated in this manner represent overall molecular motions with respect to the molecular symmetry axis.

TABLE 1: Calculation of Spin-Rotation Tensor Components for ^{13}C in Methanol

methods[a]	C_{xx} (kHz)	C_{yy} (kHz)	C_{zz} (kHz)
1	5.15[b]	4.69	12.72
	5.04[c]	4.87	13.51
2	4.86	4.51	12.45
3	4.99[b]	4.51	14.23
	4.88[c]	4.69	15.03

[a] Methods 1−3 are described in the text. [b] The solid-state chemical shift data were taken from ref 31. [c] The solid-state chemical shift data were taken from ref 32.

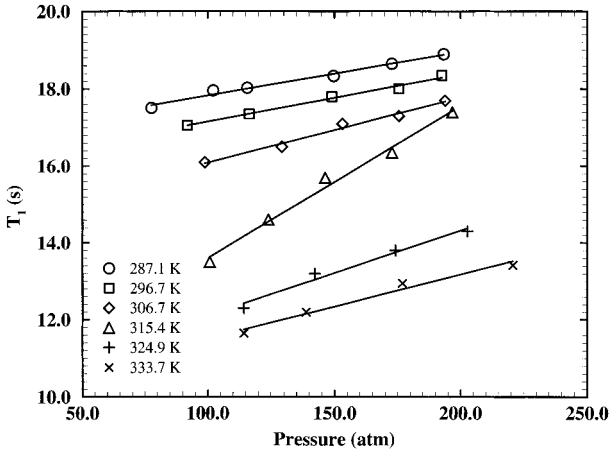

Figure 1. Spin−lattice relaxation time (T_1) isotherms as a function of pressure for 0.042 mole fraction methanol in CO_2.

Results and Discussion

A. Spin−Lattice Relaxation Times and NOE Measurements. Carbon-13 spin−lattice relaxation times (T_1) have been measured over a range of pressure from 80 to 220 atm along six isotherms distributed from 287 to 334 K. Spin−lattice relaxation times for CO_2 were simultaneously determined. Differences between CO_2 spin−lattice relaxation times in CO_2−methanol mixtures and in neat CO_2 at the same temperature and pressure were observed to be small, as expected. The carbon spin−lattice relaxation processes in CO_2 are dominated by spin-rotation interactions and have been discussed elsewhere.[16,19] T_1 isotherms for methanol are presented in Figure 1. From Figure 1, it is noted that T_1 increases slowly with increasing pressure and decreases dramatically with increasing temperature. This indicates a dominant spin-rotation contribution to the overall spin−lattice relaxation. An increase of pressure at constant temperature increases the fluid density and, therefore, increases the molecular collision frequency. This leads to a decreased angular momentum correlation time and, therefore, to a decrease in the relaxation rate R_1. At constant pressure, the spin-rotation relaxation rate increases with temperature (cf. eqs 5 and 8) so that a reduction of relaxation time is observed. Also, note in this figure that the slope of the isotherm at 315.4 K is greater than at any other temperature. This can be explained by noting that the critical temperature for this mixture is 313.2 K.[39] The NOE values measured along these isotherms were found to be independent of pressure within experimental error. The average NOE data with standard deviations are listed in Table 2 as a function of temperature. The NOE values, ranging between 1.4 and 1.8 within the temperature range, are translated into a 44−60% contribution of dipole−dipole relaxation to the total spin−lattice relaxation. The NOE values decrease as temperature increases, indicating

TABLE 2: NOE Effects and Change in Partial Molar Volume Due to Hydrogen Bond Formation for Methanol in CO_2[a]

temp (K)	NOE[b]	$\Delta\bar{V}$ cm^3/mol per hydrogen bond formed			
		trimer[c]	tetramer[c]	pentamer[c]	CSAM[d]
287.1	1.79(0.02)[e]	−35.2(4.1)	−34.9(4.0)	−34.7(4.0)	−38.9(4.6)
296.7	1.65(0.03)	−50.5(5.3)	−49.9(5.3)	−49.6(5.3)	−53.4(5.7)
306.7	1.55(0.02)	−41.2(6.8)	−40.7(6.7)	−40.4(6.7)	−43.3(6.3)
315.4	1.50(0.03)	−128.9(6.2)	−126.8(6.1)	−125.5(6.1)	−127.5(6.6)
324.9	1.50(0.05)	−69.0(2.8)	−67.6(2.7)	−66.7(2.7)	−66.4(2.5)
333.7	1.45(0.04)	−48.6(7.4)	−47.4(7.5)	−46.7(7.7)	−46.2(8.8)

[a] The mole fraction of methanol in CO_2 is 0.042. The pressure range of the measurements is from 80 to 220 atm. [b] NOE of ^{13}C in methanol as a function of temperature. The values and standard errors represent the average of measurements within the pressure ranges and their standard deviations at each temperature. No trends were observed for the NOE as a function of pressure. [c] These models assume that hydrogen-bonded oligomers are only cyclic trimers, tetramers, or pentamers, respectively. [d] CSAM stands for continuous self-association model. [e] Numbers in parentheses are standard deviations.

that the spin-rotation interactions become more important at higher temperatures.

B. Analysis of Experimental Data with Simple Spin-Rotation Relaxation Theory. The measured overall spin−lattice relaxation rate for ^{13}C in methanol can be separated into contributions from spin-rotation and dipole−dipole relaxation using the measured value of the NOE as shown in eqs 2 and 3. Simple spin-rotation relaxation theory (eqs 4, 5, and 8) described in the Theory section may also be used to calculate the spin-rotation relaxation rate, R_{SR}. The effective angular momentum correlation time, τ_J, in eq 5 is linearly related to the time, τ_{BC}, between molecular collisions. Therefore, one may calculate τ_J using gas kinetic theory. The slope of this linear relationship is proportional to an effective collision number, referred to as Z.[40] Z provides the average number of collisions needed for an effective molecular angular momentum exchange. This number is found to be between 1.4 and 3.4 for many collision pairs.[40] The effective collision number, Z, is not sensitive to changes in the partial molar volume or enthalpy. The differences in these thermodynamic properties produced by assuming that $Z = 1$ and $Z = 3$ are less than our experimental errors. For simplicity, therefore, the effective collision number of $Z = 1$ is used in the following discussion.

The expression for computing τ_J is given by[16]

$$\tau_J = (\rho\bar{\nu}\sigma_K)^{-1} \tag{13}$$

where ρ is fluid density, and $\bar{\nu}$, the average velocity of molecules, can be estimated from molecular properties of methanol and CO_2 as a function of temperature.[16] The kinetic collisional cross section, σ_K $(=\pi d^2_{CO_2-CH_3OH})$,[41] assumes $d_{CO_2-CH_3OH}$ may be treated as a geometric mean[42] of the Lennard-Jones distance parameters for pure CO_2 and methanol. These parameters are 0.3626 and 0.3941 nm for methanol and carbon dioxide, respectively.[42] Theoretical R_{SR} values, calculated using eqs 4, 5, 8, and 13, are 3−4 times larger than experimental values over the temperature and pressure ranges. This indicates that there may exist a significant number of methanol clusters that damp the spin-rotation relaxation compared to that predicted by simple kinetic theory. The theoretical values assume monomeric methanol molecules not associated with each other. This leads us to postulate that the measured spin relaxation rates are an average of methanol monomers and "solute clusters". In the case of methanol, these clusters are most likely hydrogen-bonded oligomers.

C. Hydrogen Bonding Model of Spin−Lattice Relaxation. I. The Cyclic Oligomer Model. Hydrogen-bonded alcohol association has been observed for many years. NMR chemical shift measurements have been successfully applied to explain alcohol hydrogen bonding in conventional liquid solvents, where the observed chemical shifts are considered to be the weighted average of free molecules and hydrogen-bonded complex.[8,43,44] In the hydrogen bonding model of spin−lattice relaxation, we assume that the spin relaxation rate of methanol monomers may be described using simple relaxation theory (eqs 4, 5, and 8), where both overall rotation and internal rotation contribute to the spin relaxation. However, only methyl group internal rotation contributes to the spin-rotation relaxation in the hydrogen-bonded methanol complex. This assumption is based on the fact that the contribution from overall molecular rotation becomes negligibly small when several methanol molecules are assumed to rotate as a rigid unit. However, the internal rotational motions of the methyl group are independent of complex size. If R_m and R_{cl} represent the spin-rotation relaxation rates for monomer and cluster, respectively, we have

$$R_m = R_{int} + R_{overall}$$
$$R_{cl} = R_{int} \tag{14}$$

If the cyclic oligomeric model[5] for methanol at modest concentration in a nonpolar solvent is used, one has an equilibrium as follows

$$n(CH_3OH) \leftrightarrow (CH_3OH)_n \tag{15}$$

where n is an integer between 3 and 6 and averages about 4. One can define an equilibrium constant, K_4, from eq 15 as

$$K_4 = y_4/y_1^4 \tag{16}$$

where y_1 and y_4 are the "true" mole fractions at equilibrium for monomer and tetramer, respectively. These mole fractions are related to the total methanol mole fraction, X_A, by

$$X_A = (y_1 + 4y_4)/(1 + 3y_4) \approx y_1 + 4y_4 \tag{17}$$

since the tetramer concentration is presumed to be small. It is presumed that the rate of exchange of molecules into and out of the cluster is rapid compared to spin relaxation processes. Then, spin-rotation relaxation may be expressed in terms of equilibrium mole fractions of monomer and tetramer.

$$X_A R_{SR} = y_1 R_m + 4y_4 R_{cl} \tag{18}$$

Equations 16−18 express the hydrogen-bonding model for methanol in terms of the spin-rotation relaxation data. In eq 18, R_{SR} may be obtained from experimental measurements; R_m and R_{cl} may be calculated using eqs 5, 8, and 14. The three variables y_1, y_4, and K_4 may be obtained by solving the three eqs (16−18) simultaneously. Similar equations could be written for the trimer ($n = 3$) and the pentamer ($n = 5$).

II. The Continuous Self-Association Model. The cyclic oligomer model[5] assumes that all clusters are of the same size. Details of other hydrogen-bonding structures, which most likely also exist in the mixture, are lumped into the parameter n characterizing the average cluster. This assumption appears to work well when methanol concentrations are high. In general, the continuous self-association model (CSAM)[45,46] offers a conceptually more satisfying approximation. In the CSAM, the solute molecule is in equilibrium with a series of oligomers as

follows

$$CH_3OH + CH_3OH \overset{K_2}{\leftrightarrow} (CH_3OH)_2$$

$$(CH_3OH)_2 + CH_3OH \overset{K}{\leftrightarrow} (CH_3OH)_3$$

$$(CH_3OH)_n + CH_3OH \overset{K}{\leftrightarrow} (CH_3OH)_{n+1} \qquad (19)$$

where K_2 and K are the equilibrium constants for dimer and higher oligomer formation, respectively. If mole fraction concentrations are used, these constants may be expressed as

$$K_2 = y_2/y_1^2 \qquad (20)$$

$$K = y_{n+1}/y_n y_1$$

Spin relaxation may be developed under this model by first defining variables s_1 and s_2 as

$$s_1 = \sum_i y_i$$

$$s_2 = \sum_i i y_i \qquad i = 1, 2, ... \qquad (21)$$

where y_i is the "true" mole fraction for oligomer i. The relationship between the mole fraction X_A and the variable defined above is

$$X_A = s_2/(1 - s_1 + s_2) \qquad (22)$$

By substituting eq 20 into eq 21, s_1 and s_2 may be rewritten as

$$s_1 = y_1 + \frac{K_2 y_1^2}{1 - K y_1} \qquad (23a)$$

$$s_2 = y_1 \frac{ds_1}{dy_1} = y1 + \frac{K^2 y_1^2 (2 - K y_1)}{(1 - K y_1)^2} \qquad (23b)$$

Equation 14 is then used to determine the relaxation rate expression for the CSAM hydrogen-bonding model:

$$X_A R_{SR} = y_1 R_m + (s_2 - y_1) R_{cl} \qquad (24)$$

The hydrogen bond model expressed in this manner does not distinguish between the linear and cyclic aggregates. It has been reported that cyclic oligomeric structures are more stable than linear ones for methanol.[5,8] Hence, it is assumed that the cyclic structures for the hydrogen-bonded complexes are dominant in the mixture. Note, there are five variables (s_1, s_2, y_1, K_2, and K) in this model with only four independent equations (cf. eqs 22, 23, and 24). To resolve this problem, it is assumed that the mole fraction of the dimeric complex is small compared to the cyclic oligomer complexes, and K_2 is negligible. This issue will be addressed in detail in the next section.

D. Thermodynamics of the CO_2−Methanol Mixture. The partial molar volume change, $\Delta\bar{V}$, for hydrogen bond aggregation processes is defined by

$$\Delta\bar{V} = -RT(\partial \ln K/\partial P) \qquad (25)$$

$\Delta\bar{V}$ represents the difference in molar volumes of methanol hydrogen-bonded complexes from the molar volume of the methanol monomer. The derivatives of equilibrium constants, K, with respect to temperature give the change of partial molar enthalpy as a consequence of hydrogen-bonded complex formation, $\Delta\bar{h}_{HB}$.

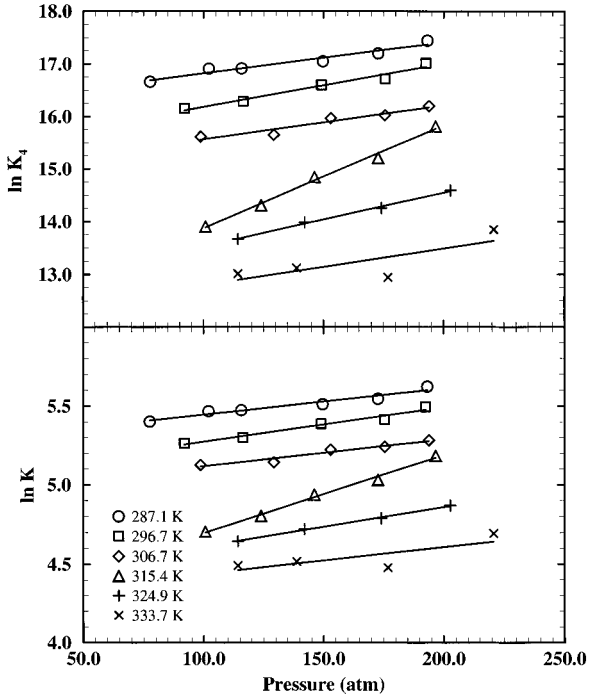

Figure 2. Pressure dependence of equilibrium constants for hydrogen bond formation. Top: pressure dependence of ln K_4 for six isotherms. Bottom: pressure dependence of ln K for six isotherms. See text for a discussion of the kinetic models involved.

$$\Delta\bar{h}_{HB}/RT^2 = -(\partial \ln K/\partial T) \qquad (26)$$

$\Delta\bar{h}_{HB}$ involves the enthalpy term solution effects[5] since the standard state chosen here is pure methanol monomer instead of the ideal gas standard state.

The data will first be analyzed using the cyclic oligomeric hydrogen-bonding model (eqs 16−18). The upper part of Figure 2 shows the pressure dependence of ln(K_4) along six spin−lattice relaxation time isotherms. The $\Delta\bar{V}$ data may be extracted from the slopes of these plots. Similar plots are obtained for the trimeric and pentameric models, and these results are summarized in Table 2. From Table 2, we note that the $\Delta\bar{V}$ values are negative at all temperatures. Evidently, hydrogen bonding is accompanied by a decrease in volume.[47] The decrease of $\Delta\bar{V}$ is probably due to the contraction of solute volume from approximately four methanol monomers to a single aggregated tetramer.[5] As suggested by Smith et al., the solvent clustering around an aggregate might also contribute to this large volume decrease. A striking features of $\Delta\bar{V}$ for this mixture is shown in Figure 3 by plotting $\Delta\bar{V}$ of the tetrameric model vs temperature. The volume contraction is substantially greater around 315 K, close to the critical temperature of 313 K[39] for this mixture. According to pioneering work by Eckert et al.,[48] the partial molar volume of naphthalene in CO_2 decreases by 7.8 L/mol near the critical point, and the solvent (CO_2) isothermal compressibility is highly correlated with this volume change. A large decrease in the partial molar volume (1.4 L/mol) was observed for the equilibrium of 2-hydroxypyridine with 2-pyridone in supercritical fluids by Johnston et al.[49] The energy evolved in hydrogen bond formation is substantially less than that involved in formation of a covalent bond. A partial molar volume change of −126 mL/mol per hydrogen bond observed for methanol in CO_2 near the critical point seems reasonable.

Using the best fit lines for each temperature as shown in Figure 2, values of ln(K_4) were calculated at 120, 150, and 200

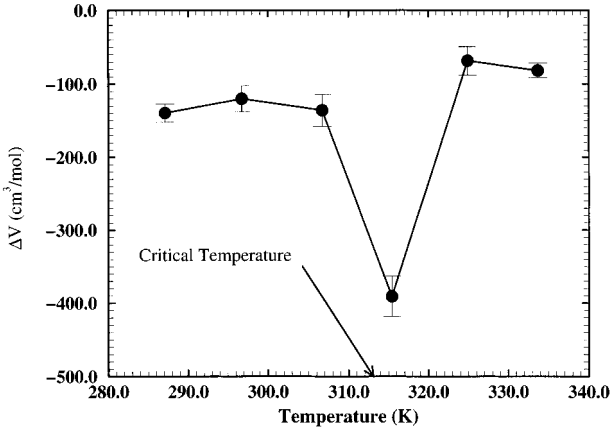

Figure 3. Partial molar volume changes for formation of hydrogen-bonded methanol tetramers plotted vs sample temperature. The observed effect is dramatically different near the critical temperature.

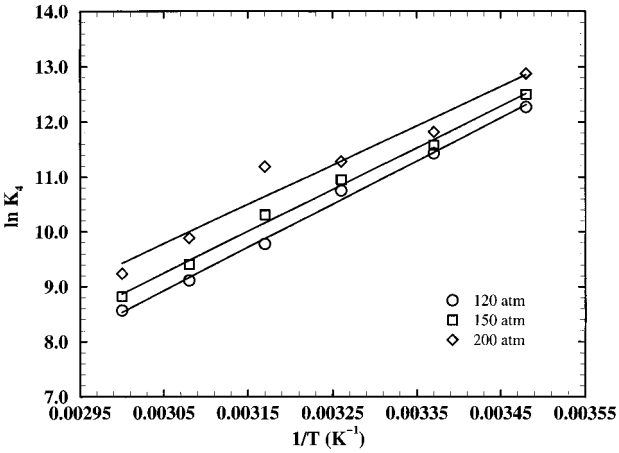

Figure 4. Equilibrium constants, ln(K_4), plotted as a function of temperature for pressures of 120, 150, and 200 atm, respectively. The partial molar enthalpy changes for tetramer formation may be obtained from these plots.

TABLE 3: Partial Molar Enthalpy Changes of Hydrogen Bonding for Methanol in CO_2[a]

	$\Delta\bar{h}_{HB}$ per hydrogen bond (kcal/mol)			
press. (atm)	trimer[b]	tetramer[b]	pentamer[b]	CSAM[c]
120.0	−4.3(0.3)[d]	−4.3(0.3)	−4.1(0.4)	−4.2(0.3)
150.0	−4.3(0.3)	−4.1(0.4)	−4.2(0.3)	−4.2(0.3)
200.0	−4.4(0.4)	−3.9(0.5)	−4.3(0.6)	−4.0(0.5)

[a] The mole fraction of methanol in CO_2 is 0.042. [b] These models assume that hydrogen-bonded oligomers are only cyclic trimers, tetramers, or pentamers, respectively. [c] CSAM stands for continuous self-association model. [d] Numbers in parentheses are standard deviations.

atm. These values are presented in Figure 4 as van't Hoff plots. From the slope of the plots, hydrogen bond enthalpies, $\Delta\bar{h}_{HB}$, are obtained and are tabulated in Table 3, together with those obtained similarly from trimer and pentamer models. The $\Delta\bar{h}_{HB}$ value of −3.9 kcal/mol obtained at 200 atm agrees well with that of −3.5 kcal/mol obtained at 197.3 atm with a methanol mole fraction of 0.072 by Smith et al.[5] The data at 200 atm for the trimer and pentamer models are also comparable with those of Smith. In general, $\Delta\bar{h}_{HB}$ values reported here and by Smith et al.[5] are lower in magnitude than values obtained from thermal conductivity measurements (−6.0 kcal/mol)[50] and ab initio calculations (−7.4 kcal/mol)[51] for the cyclic tetramer model in gas phase. However, if the differences in thermodynamic properties, such as density and diffusitivity, between a supercritical fluid and a gas phase are considered, the decrease in $\Delta\bar{h}_{HB}$ may be rationalized. Smith et al.[5] also suggest that

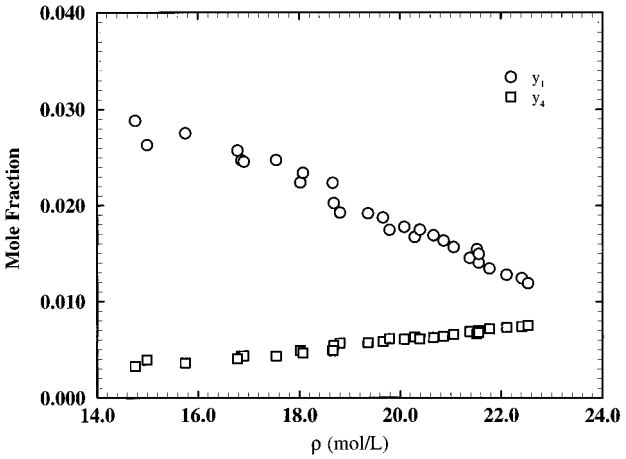

Figure 5. "True"mole fractions for the monomers and tetrameters vs density of the CO_2−methanol mixture. A reduction of y_1 and an increase of y_4 are noted at higher densities, indicating that tetrameters are favored at these densities.

solvation of methanol by CO_2 also contributes to a reduction in the magnitude of $\Delta\bar{h}_{HB}$.

Spin−lattice relaxation measurements at a variety of temperatures and pressures allow one to compare the mole fractions of methanol monomers and hydrogen-bonded cyclic aggregates in this mixture. An example of monomer−tetramer clustering is shown in Figure 5, where the mole fractions y_1 and y_4 are plotted vs fluid density. As the fluid density increases, mole fraction of monomer decreases dramatically, and the mole fraction of the tetramer increases. It is reasonable to presume that the tetramers, with their lower molar volume, are favored at higher densities, consistent with principles governing chemical equilibrium.

The continuous self-association model yielded results substantially the same as those already presented assuming specific hydrogen-bonded oligomers. As mentioned above, the dimer formation constant K_2 in this model is assumed to be negligible because ab initio calculations indicate higher stability for the cyclic oligomers. It was found in this study that K approaches an asymptote for decreasing K_2, so that the exact value chosen for K_2 becomes unimportant as long as K_2 is small. In other words, the equilibrium constant K may be obtained as the limit as K_2 approaches zero. With this approximation, the values of K have been calculated over the entire range of temperature and pressure. The pressure dependence of ln(K) at six isotherms is given in the bottom part of Figure 2. The partial molar volume changes with temperature are listed as the entries of CSAM model in Table 2. It is interesting to note that the $\Delta\bar{V}$ values from the CSAM model agree well with those from the oligomer models. Using the same procedures as above, the $\Delta\bar{h}_{HB}$ values from the CSAM model have been determined and are tabulated in Table 3. It is obvious that the good agreement between the CSAM model and the single oligomer models stems in part from the assumption that the linear dimer concentration is negligible.[8,43] The CSAM model permits all oligomers rather than restricting the model to a single oligomer, but either model predicts essentially the same molar volume changes and enthalpy changes. Thus, some sort of aggregation explains the spin-rotation relaxation data, but the exact nature of the aggregation is yet unknown.

Conclusion

Spin-rotation interactions are the dominant mechanisms in the overall spin−lattice relaxation of ^{13}C in methanol dissolved in CO_2 in both supercritical and subcritical density regions, especially at higher temperature. The spin-rotation tensor

components for ^{13}C in methanol in the principal axis system of the inertia tensor are estimated to be 4.99, 4.51, and 14.23 kHz for C_{xx}, C_{yy}, and C_{zz}, respectively, based on results from solid-state chemical shift measurements. Simple spin-rotation relaxation theory assuming no aggregation of the methanol is inadequate to describe the spin-rotation relaxation rates of ^{13}C in methanol in CO_2. A hydrogen-bonding model of spin-rotation relaxation (eqs 14 and 18), proposed in this paper, is coupled with formation of hydrogen bonds to produce a single oligomer (eq 15). Changes in partial molar volumes $\Delta\bar{V}$ and enthalpies $\Delta\bar{h}_{HB}$ are then calculated. The resulting $\Delta\bar{h}_{HB}$ values compare favorably with the literature. Therefore, this model provides a basis for relaxation studies of hydrogen-bonding alcohols in supercritical fluids. The nuclear spin relaxation data show that hydrogen-bonding aggregation increases at higher densities. An anomalously large negative $\Delta\bar{V}$ is observed near the critical temperature, indicating an extreme solvent effect on hydrogen bond formation. A continuous self-association model permitting various oligomers is also used to interpret the relaxation rate data for this mixture. The fact that results are identical within experimental errors indicates that the use of the oligomer model in these systems is a good approximation. The hydrogen bond model of the spin−lattice relaxation is used to verify the dominant tetrameric structure of methanol in carbon dioxide expected from chemical shift measurements of alcohol in apolar solvents. In addition, this model quantifies thermodynamic properties such as partial molar enthalpy and partial molar volume involved in the tetramer formation.

Acknowledgment. Helpful discussions with Prof. Cynthia J. Jameson on estimation of the components of the spin-rotation interaction tensor of methanol are greatly appreciated. This work was supported at the University of Utah by Basic Energy Sciences at DOE through Grant DE FG02-94ER14452. This work is also supported at Los Alamos National Laboratory by the EPA Environmental Technologies Initiative through Grant EPA/IAG DW89936500-01.

References and Notes

(1) Dobbs, J. M.; Wong, J. M.; Lahiere, R. J.; Johnston, K. P. *Ind. End. Chem. Res.* **1987**, *26*, 56−65. (b) Dobbs, J. M.; Johnston, K. P. *Ind. End. Chem. Res.* **1987**, *26*, 1476−1482. (c) Compbell, R. M.; Djordjevic, N. M.; Markides, K. E.; Lee, M. L. *Anal. Chem.* 1988, *60*, 356−362.

(2) Davis, P. A.; Novotony, M. *J. Chromatogr.* **1988**, *452*, 623−629.

(3) Lee, M. L., Markides, K. E., Eds. *Analytical Supercritical Fluid Chromatography and Extraction*; Chromatography Conferences, Inc.: UT, 1990.

(4) Frye, S. L.; Yonker, C. R.; Kalkwarf, D. R.; Smith, R. D. In *Supercritical Fluids*; ACS Symposium Series 329; Squires, T. G., Paulaitis, M. E., Eds.; American Chemical Society: Washington, DC, 1987.

(5) Fulton, J. L.; Yee, G. G.; Smith, R. D. *J. Am. Chem. Soc.* **1991**, *113*, 8327−8334.

(6) Badger, R. M.; Bauer, S. H. *J. Chem. Phys.* **1937**, *5*, 839−851.

(7) Fletcher, A. N. *J. Chem. Phys.* **1972**, *76*, 2562−2571.

(8) Karachewski, A. M.; Howell, W. J.; Eckert, C. A. *AIChE J.* **1991**, *37*, 65−73.

(9) Pfund, D. M.; Zemanian, T. S.; Linehan, J. C.; Fulton, J. L.; Yonker, C. R. *J. Phys. Chem.* **1994**, *98*, 11846−11857.

(10) Nishikawa, K.; Tanaka, I.; Amemiya, Y. *J. Phys. Chem.* **1996**, *100*, 418−421.

(11) Ying, Q.; Wu, G.; Chu; B.; Farinto, R.; Jackson, L. *Macromolecules* **1996**, *29*, 4646−4654.

(12) Low, P. M. N.; Yong Y. L.; Yan, Y. K.; Andy Hor, T. S.; Lam, S-L.; Chan, K. K.; Wu, C.; Au-Yeung, S. C. F.; Wen, Y.-S.; Liu, L.-K. *Organometallics* **1996**, *15*, 1369−1375.

(13) Grant, D. M.; Mayne, C. L.; Liu, F.; Xiang, T. X. *Chem. Rev. (Washington, D.C.)* **1991**, *91*, 1591−1624.

(14) Lamb, D. M.; Adamy, S. T.; Woo, K. W.; Jonas, J. *J. Phys. Chem.* **1989**, *93*, 5002−5005.

(15) Jonas, J. In *NMR, Basic Principles and Progress 24: High-Pressure NMR*; Diehl, P., Fluck, E., Gümther, H., Kosfeld, R., Seelig, J., Eds.; Springer-Verlag: Berlin, 1991.

(16) Etesse, P.; Zega, J. A.; Kobayashi, R. *J. Chem. Phys.* **1992**, *97*, 2022−2029.

(17) Etesse, P.; Ward, A. M.; Kobayashi, R. *Physica B* **1993**, *183*, 45−52.

(18) Etesse, P.; Chapman, W. G.; Kobayashi, R. *Mol. Phys.* **1993**, *80*, 1145−1164.

(19) Bai, S.; Mayne, C. L.; Pugmire, R. J.; Grant, D. M. *Magn. Reson. Chem.* **1996**, *34*, 479−488.

(20) Bai, S.; Mayne, C. L.; Taylor, C. M.; Liu, F.; Pugmire, R. J.; Grant, D. M. *J. Phys. Chem. B* **1997**, *101*, 2923−2928.

(21) Bai, S.; Mayne, C. L.; Taylor, C. M.; Pugmire, R. J.; Grant, D. M. *Rev. Sci. Instrum.* **1995**, *67*, 240−243.

(22) Dunkel, R. U.S. Patent 5,218,299, Jan 8, 1993.

(23) Harris, R. K. *Nuclear Magnetic Resonance Spectroscopy*; The Bath Press: Avon, 1986; Chapter 4.

(24) SF−Solver: Software for Supercritical Fluid Analysis, Isco, Inc., Lincoln, NE.

(25) Jameson, C. J. *Chem. Rev. (Washington, D.C.)* **1991**, *91*, 1375−1395.

(26) McClung, R. E. D. In *Encyclopedia of NMR*; Grant, D. M., Harris, R. K., Eds.; Wiley: London, 1996; pp 4530−4535 and references therein.

(27) Armstrong, B. L.; Courtney, J. *Can. J. Phys.* **1972**, *50*, 1262−1272.

(28) The overall part of the spin-rotation relaxation rate involves three correlation times: τ_1, τ_{12}, and $\tau_{12'}$. τ_1 and τ_{12} are the reorientational correlation times of the molecular angular momentum changes and are proportional to each other. $\tau_{12'}$ is a time that measures the rigidity of angular momentum identified with the molecular symmetry axis. The angular momentum reorients with the molecular symmetry axis during a collision as one assumes that $\tau_{12'} = \tau_1$. If an assumption is made that all three correlation times are the same[27] and are designated as an effective spin-rotation correlation time, τ_J, the relaxation rate due to spin rotation of overall molecular motions may be simplified to be a function of a single correlation time.

(29) De Lucia, F. C., Herbst, E., Anderson, T. *Astrophys. J. Suppl. Ser.* **1987**, *64*, 703−714.

(30) Jameson, C. J.; Jameson, A. K.; Smith, N. C.; Jackowski, K. *J. Chem. Phys.* **1987**, *86*, 2717−2722.

(31) Spiess, H. W.; Schweitzer, D.; Haeberlen U. *J. Magn. Reson.* **1973**, *9*, 444−460.

(32) Burke, T. E.; Chan, S. I. *J. Magn. Reson.* **1970**, *2*, 120−140.

(33) Gaisin, N. K.; Manyurov, I. R.; Enikeen, K. M.; Il′yasor, A. V. *Chem. Phys. Rep.* **1995**, *13*, 1348−1358.

(34) Yi, P. N.; Ozier, I.; Ramsey, N. F. *J. Chem. Phys.* **1971**, *55*, 5215−5227.

(35) Jameson, C. J. Private communications, 1995.

(36) (a) Flygare, W. H. *Chem. Rev. (Washington, D.C.)* **1974**, *74*, 653−687. (b) Gierke, T. D.; Flygare, W. H. *J. Am. Chem. Soc.* **1972**, *94*, 7277−7283.

(37) Solum, M. S.; Facelli, J. C.; Michl, J.; Grant, D. M. *J. Am. Chem. Soc.* **1986**, *108*, 6464−6470.

(38) Pines, A.; Gibby, M. G.; Waugh, J. S. *Chem. Phys. Lett.* **1972**, *15*, 373

(39) Gurdial, G. S.; Foster, N. R.; Yun, J. S. L. In *Proceeding of the 2nd International Symposium on Supercritical Fluids*, McHugh, M. A., Ed.; Johns Hopkins University: Baltimore, MD, 1991.

(40) Maryott, A. A.; Malmberg, M. S.; Gillen, K. T. *Chem. Phys. Lett.* **1974**, *25*, 169−174.

(41) Jameson, C. J.; Jameson, A. K.; Smith, N. C.; Hwang, J. K; Zia, T. *J. Phys. Chem.* **1991**, *95*, 1092−1098.

(42) Reid, R. C.; Sherwood, T. K. *The Properties of Gases and Liquids*; McGraw-Hill Book Co.: New York, 1966; Chapter 7.

(43) Gutowsky, H. A.; Saike, A. *J. Chem. Phys.* **1953**, *21*, 1688−1694.

(44) Karachewski, A. M.; McNeil, M. M.; Eckert, C. A. *Ind. Eng. Chem. Res.* **1989**, *28*, 315.

(45) Bartczak, W. M. *Ber. Bunsen-Ges. Phys. Chem.* **1979**, *83*, 987−992.

(46) Aveyard, R.; Briscoe, B. J.; Chapman, J. *J. Chem. Soc., Faraday Trans. 1* **1973**, *69*, 1772−1798.

(47) Isaacs, N. S. *Liquid-Phase High-Pressure Chemistry*, John Wiley & Sons: Chichester, 1981; Chapter 3.

(48) Eckert, C. A.; Ziger, D. H.; Johnston. K. P.; Kim, S. *J. Phys. Chem.* **1986**, *90*, 2738−2746.

(49) Peck, D. G.; Mehta, A. J.; Johnston. K. P. *J. Phys. Chem.* **1989**, *93*, 4297−4304.

(50) Renner, T. A.; Kucera, G. H.; Blander, M. *J. Chem. Phys.* **1977**, *66*, 177−184.

(51) Curtiss, L. A. *J. Chem. Phys.* **1977**, *67*, 1144−1149.